引用格式：WANG Hao, FU Yue-gang, ZHANG Guo-yu, *et al*. Concentration Performance Analysis of Solar Simulator Based on Compound Parabolic Concentrator[J]. *Acta Photonica Sinica*, 2020, **49**(12):1223001
王昊,付跃刚,张国玉,等.基于CPC的太阳模拟器聚光性能分析[J].光子学报,2020,**49**(12):1223001

基于CPC的太阳模拟器聚光性能分析

王昊[1],付跃刚[1],张国玉[1,2],孙高飞[1,2],刘石[1,2],张健[1,2],徐达[1,2],吴凌昊[1,2],杨俊杰[1,2]

(1 长春理工大学 光电工程学院,长春 130022)
(2 吉林省光电测控仪器工程技术研究中心,长春 130022)

摘 要:为解决现有太阳模拟器能量利用率低导致辐照度低的难题,依据太阳模拟器基本成像原理,提出利用复合抛物面聚光器(CPC)改进太阳模拟器的聚光系统.分析了CPC与传统聚光器的聚光机理,基于边缘光线原理推导了CPC的参数设计方法.利用LightTools软件结合嵌套的体光源与CPC建立聚光模型,分析了CPC理想最大接收角。建立椭球聚光镜与组合聚光系统的对比模型,验证了理论分析.通过截取分析得到最佳截取比来优化初始结构,进而确定CPC的最终结构.结果表明:氙灯应用在CPC中的能量利用率高达94.86%,且整个太阳模拟器的辐照度有很大提升.该研究能够为设计高能量利用率高辐照度的太阳模拟器提供参考.

关键词:太阳模拟器;复合抛物面聚光器;能量利用;聚光系统;辐照度;椭球聚光器;辐照均匀度
中图分类号:V19 **文献标识码**:A **doi**:10.3788/gzxb20204912.1223001

Concentration Performance Analysis of Solar Simulator Based on Compound Parabolic Concentrator

WANG Hao[1], FU Yue-gang[1], ZHANG Guo-yu[1,2], SUN Gao-fei[1,2], LIU Shi[1,2], ZHANG Jian[1,2], XU Da[1,2], WU Ling-hao[1,2], YANG Jun-jie[1,2]

(1 *College of Optoelectronic Engineering, Changchun University of Science and Technology, Changchun* 130022, *China*)
(2 *Optical Measurement and Control Instrumentation, Jilin Province Engineering Research Center, Changchun* 130022, *China*)

Abstract: To solve the problem of low irradiance caused by the low energy utilization rate of an existing solar simulator, a Compound Parabolic Concentrator (CPC) based on the basic imaging principle of the solar simulator was proposed to improve the concentrating system of the simulator. The condensing mechanism of the CPC and a traditional condenser was analyzed, and the parameter design method of the CPC was derived based on the edge-ray principle. Using the LightTools software combined with a nested body light source and the CPC to build a condenser model, the ideal maximum receiving angle of the CPC was analyzed. A comparison model between the ellipsoidal condenser and the combined condenser system

Foundation item: "Thirteenth Five-Year" Science and Technology Project of Jilin Provincial Department of Education (No. JJKH20181131KJ), Jilin Scientific and Technological Development Program (No.20190302124GX), Science and Technology Innovation Fund of Changchun University of Science and Technology (No.XJJLG-2018-02), Jilin Scientific and Technological Development Program (No.20200602055ZP)

First author: WANG Hao (1997—), male, M.S. degree, mainly focuses on aerospace ground simulation. Email:2276274879@qq.com
Supervisor (Contact author): FU Yue-gang (1972—), male, professor, Ph.D. degree, mainly focuses on advanced optical system and bionic optics. Email:fuyg@cust.edu.cn

Received: Aug.6,2020; **Accepted**: Sep.30,2020

was established to verify the theoretical analysis. The optimal intercept ratio was obtained through an intercept analysis to optimize the initial structure and to determine the final structure of the CPC. Results show that the energy utilization rate of xenon lamps used in the CPC is as high as 94.86%. Furthermore, the irradiance of the entire solar simulator can be greatly improved. The findings of this study present a reference for designing highly energy efficient and high-irradiance solar simulators.

Key words: Solar simulator; Compound parabolic concentrator; Energy utilization; Concentrating system; Irradiation; Ellipsoid condenser; Uniformity of irradiation

OCIS Codes: 230.2090; 080.2740; 080.4295; 080.4298

0 Introduction

A solar simulator is a radiation of equipment capable of producing light sources with characteristics similar to the geometrical and irradiation features of the sun. The optical system of simulator comprises a light source, a condensing system, a uniform light system, and a collimating system. The light source typically employs a xenon lamp with an output that matches the solar spectrum. The condensing system uses an ellipsoidal condensing mirror. An optical integrator is used in the uniform light system. These systems are matched with one another to realize the solar radiation simulation. This approach is widely used and is important in the aerospace, meteorological, and photovoltaic industries, among others.

A Compound Parabolic Concentrator (CPC) is generally used as a heat collector in the field of solar energy[1] and also prominently contributes to the field of lighting[2]. ANDREEV V proposed using a convex lens and CPC to form a two-stage concentrator for power generation, wherein the optical efficiency reached 90%[3]. HU Pian et al. optimized a CPC in a solar laser, wherein the total light collection efficiency reached 50.4%[4]. POTTAS J and others designed a CPC that was applied to a multisource high-flux solar simulator, achieving an optical efficiency of 85.4%, and its CPC concentration ratio increased by 4.1 times, which was able to reduce the irradiation nonuniformity[5]. In summary, a CPC can significantly improve the optical efficiency. The combination of a CPC and a spherical reflector can greatly improve the irradiance of the solar simulator.

Research on the design method of the compound parabolic concentrator used in a solar simulator, the CPC was designed based on the edge ray principle. The optical system's simulation model was established using LightTools. The light collection efficiency of the simulated beam in the CPC and the ellipsoidal condenser was compared and analyzed. The problem of low energy utilization in solar simulators presents new ideas for the research on concentrating systems.

1 Composition and working principle of solar simulator optical system

The solar simulator employs a coaxial transmission collimation system. The optical system mainly comprises a xenon lamp, a concentrating system (a spherical reflector and the CPC), a shaping system, an optical integrator, a diaphragm, and a collimation lens group, as shown in Fig. 1.

A short-arc xenon lamp is used as the light source for the solar simulator. The luminous xenon arc between the cathode and anode of the xenon lamp is placed at the focal plane of the CPC. The light emitted by the xenon

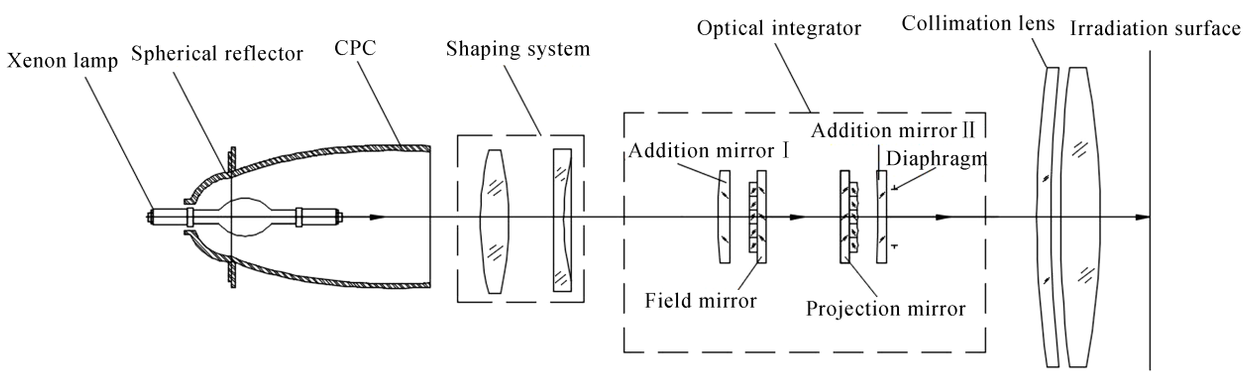

Fig. 1 Overall layout of the solar simulator

lamp exits the spherical reflector and the CPC. Then, the outgoing light beam is projected onto the optical integrator through the lens. In the integrator, the light beam is divided by the field mirror and then superimposed and imaged by the projection mirror. The light beam is projected onto the irradiation surface through the diaphragm and the collimation lens group to form a uniform and collimated light spot, thus achieving the simulating solar irradiation.

2 Design of concentrating system

Based on the path reversal principle, the CPC is designed as a reflective glass. The light source is placed in the exit hole; the light then exits the entrance hole at a particular angle and the addition of a spherical reflector prevented the loss of direct backward light from and made effective use of it. The CPC can achieve the maximum theoretical concentration ratio[6] and could be employed in the light-concentration system of the solar simulator to improve the energy utilization of the light source.

The light collection efficiency of the ellipsoidal condenser and the CPC can be calculated using the ratio of the radiant flux received by the irradiated surface to the radiant flux emitted by the light source, as shown below in Eq. (1).

$$K_c = \frac{2\pi \int_{u_0}^{u_m} t(u) \sin u \mathrm{d}u}{2\pi \int_0^{180^\circ} t(u) \sin u \mathrm{d}u} \tag{1}$$

where K_c is the concentrating efficiency, $t(u) = I/I_0$ indicates the relative distribution of the irradiance of the light source in different directions, I_0 is the normal luminous intensity of the light source, I is any light intensity in the direction of angle u with the light source axis, and u_0 and u_m are the containment angles. The above equation indicated that the light collection efficiency differed under different containment angles. The maximum containment angle of the ellipsoidal condenser was 30°~135°[7]. The containment angle can be obtained based on the luminous intensity distribution curve of the light source.Except for the reflected light, a large degree of light from the light source can not reach the second focal point when they are directly irradiated, which results in the loss of part of the light and reduces the light collection efficiency of the ellipsoidal mirror. After the intercepted part of the designed CPC, the calculation found that its containment angle was still larger than that of the ellipsoidal mirror. Accordingly, more light is used and CPC's light collection efficiency may be much higher compared with that of the ellipsoidal mirror.

2.1 Concentrating principle of CPC

The CPC's concentrating principle is edge ray principle. For a light beam entering a large aperture of the CPC at the maximum incidence angle, the edge light must exit from the edge of the small aperture; that is, the light emitted from the edge of the light source should reach the edge of the target. As shown in Fig.2, the AB segment in the parabola is intercepted and rotated around the central axis OY' to form a three-dimensional CPC.

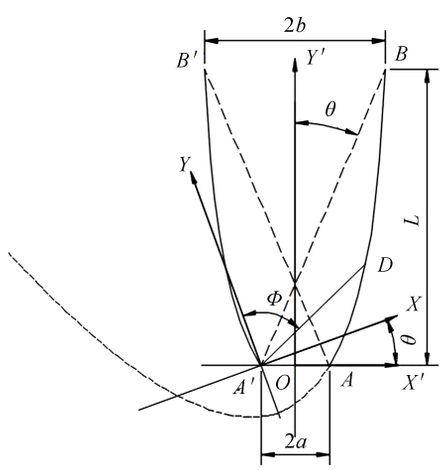

Fig. 2 Diagram illustrating the CPC's concentrating principle

Point A' is the focus of parabola AB and point A is the focus of parabola $A'B'$. The focal points of the two curves are not at the same point. As such, this is a nonconfocal system in the context of nonimaging optics[8]. The angle θ between AB' and the central axis indicats the maximum acceptance angle, and AB' as the edge ray is parallel to the Y-axis of the symmetrical axis of the parabola. The diameter of the entrance aperture BB' is $2b$, the diameter of the exit aperture AA' is $2a$, and the length of the CPC is L. When the incident angle of light entering BB' is less than or equal to θ, all the light exits from AA' following reflection. When the incident angle is greater than θ, the light exits from BB' after multiple reflections.

Analysis of Fig.2 provided an understanding of the relationship between the parameters and facilitation of the overall design. The equation for parabolic AB is expressed as Eq. (2).

$$\left[2\sqrt{2af-f^2}\,x+2(f-a)y\right]^2+8af^2x-8a(f+a)\sqrt{2af-f^2}\,y=4fa^2(f+2a) \tag{2}$$

when $x=b$, then $y=L$, then Eq. (3) below can be derived from Eq. (2).

$$b=\frac{L(a-f)\sqrt{2af-f^2}-af^2+2a\sqrt{af\left(L\sqrt{2af-f^2}+af\right)}}{f(2a-f)} \tag{3}$$

Eq.(3) enables deriving the relationship between the entrance aperture and the length of the CPC[9]. The focal length was determined through the maximum receiving angle. When the length of the CPC is longer, the containment angle was observed to be larger and more light could be reflected. Accordingly, the irradiance of the solar simulator was improved.

2.2 Parameter design of the CPC

With an understanding of the working principle of the CPC, to conveniently establish a CPC model, the calculation formula of each parameter was deduced. The CPC in the $X'OY'$ rectangular coordinate system was extracted into the polar coordinate system $XA'Y$, and the parabolic polar coordinate equation was used to analyze the CPC's parameter design[10], as shown in Fig.3.

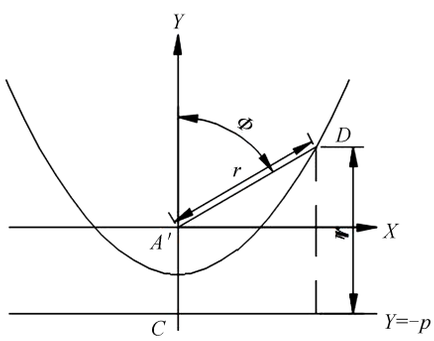

Fig. 3 Polar coordinate equation diagram

In Fig.3, D is an arbitrary point on the parabola, A' is the focus of the parabola, and the straight line is the guideline of the parabola. The focal length of the parabola is $f=\frac{p}{2}$ and the equation of the parabola is $y=\frac{1}{4f}x^2$.

Using the definition of the parabola, the distance from any point on the parabola to the fixed point was equal to the distance from the point to the fixed line, and Eq. (4) below could be obtained.

$$r-p=r\sin\left(\frac{\pi}{2}-\varphi\right)\Rightarrow r=\frac{p}{1-\cos\varphi}=\frac{2f}{1-\cos\varphi} \tag{4}$$

In Eq.(4), r is the distance of $A'D$ and$\varphi$is the angle between $A'D$ and the Y-axis.when $r=2a$, then $\varphi=\frac{\pi}{2}+\theta$, substituting Eq. (4) can deduce that the maximum receiving angle satisfies Eq. (5).

$$\theta=\arcsin\left(\frac{f}{a}-1\right) \tag{5}$$

The length L of the CPC obtained by the sine theorem is shown in Eq. (6).

$$L = \frac{bf\cos\theta}{a\sin\theta} \tag{6}$$

when a and θ are determined, the parameters f, b, and L can be obtained from Eq. (6), and a can be obtained from Eq. (7) below. Following the simulation analysis, the ideal θ angle was obtained. Following this design process, the geometric structure of the CPC was determined.

The exit aperture of the CPC had to support the installation of the xenon lamp light source and ensure a degree of radial adjustment margin, as shown in Eq. (7)[11].

$$a \geqslant \frac{d}{2} + \Delta \tag{7}$$

In Eq. (7), d is the shell diameter of the selected xenon lamp (60 mm) and Δ is the radial adjustment margin (2 mm). Then, $a \geqslant 32$ mm is obtained (32 mm), and the exit aperture is determined as being 64 mm.

2.3 Design of the spherical mirror

The spherical mirror was designed based on the CPC parameters. Its radius had the same parameters as that of exit aperture of the CPC. The center of the sphere was located at the light source. The lower aperture and the upper aperture had to satisfy Eq. (8). The xenon lamp could be placed between the combined mirrors to realize the effective use of the light beam.

$$\begin{cases} d_1 \geqslant h_1 \\ d_2 = a \end{cases} \tag{8}$$

In Eq. (8), d_1 is the aperture of the lower opening of the spherical reflector, h_1 is the diameter of the xenon lamp holder, and d_2 is the aperture of the upper opening of the spherical reflector.

3 Simulation analysis

Analysis and study of the utilization of the CPC in the solar simulator, alongside a sensible design of the CPC′s external dimensions, effectively improved the energy utilization of the light source. Using the LightTools software, a physical model of the CPC was created and the ideal acceptance angle was analyzed and determined. The CPC profile parameters calculated in the above equations were used as input, suitable materials and surface properties were determined, and the optimal interception ratio was selected to simplify the CPC′s overall structure.

3.1 Light source modeling

A short-arc xenon lamp is typically used as the light source for a solar simulator. Its advantage is that the spectral distribution of the xenon lamp is close to that of actual sunlight, exhibits strong stability[12], provides the symmetrical distribution of the light distribution curve, and the cathode spot is similar to the point light source, which is conducive to the design of the optical system. After calculation, a 4500-W xenon lamp was selected as the light source for the solar simulator.

Based on the lamp brightness curve in LightTools, the light-emitting area of the xenon lamp was divided into three parts, three sub-light source models were used to simulate the light emission of the three subareas, and a certain proportion of power was allocated. The volume light source model is shown in Fig.4.

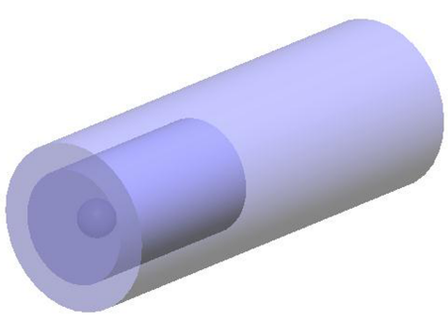

Fig. 4 Xenon lamp body light source model

3.2 CPC′s simulation modeling

The main method of measuring the performance of the condenser was to analyze its optical efficiency, that is, to transmit a high percentage of the light emitted from the front surface to the exit hole[13]. To model the CPC in LightTools, when the exit aperture was the same, comparative analysis of the CPC at different receiving angles (0°, 10°, 15°, and 30°) was conducted to determine the ideal receiving angle. Results are shown in Fig.5. Fig. 6 presents the simulation grid results.

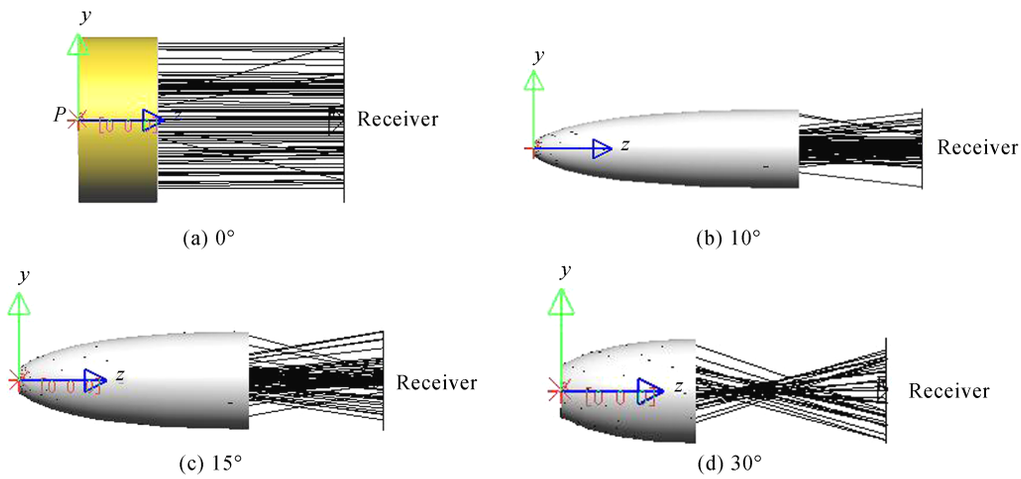

Fig. 5 CPC simulation graph under different receiving angles

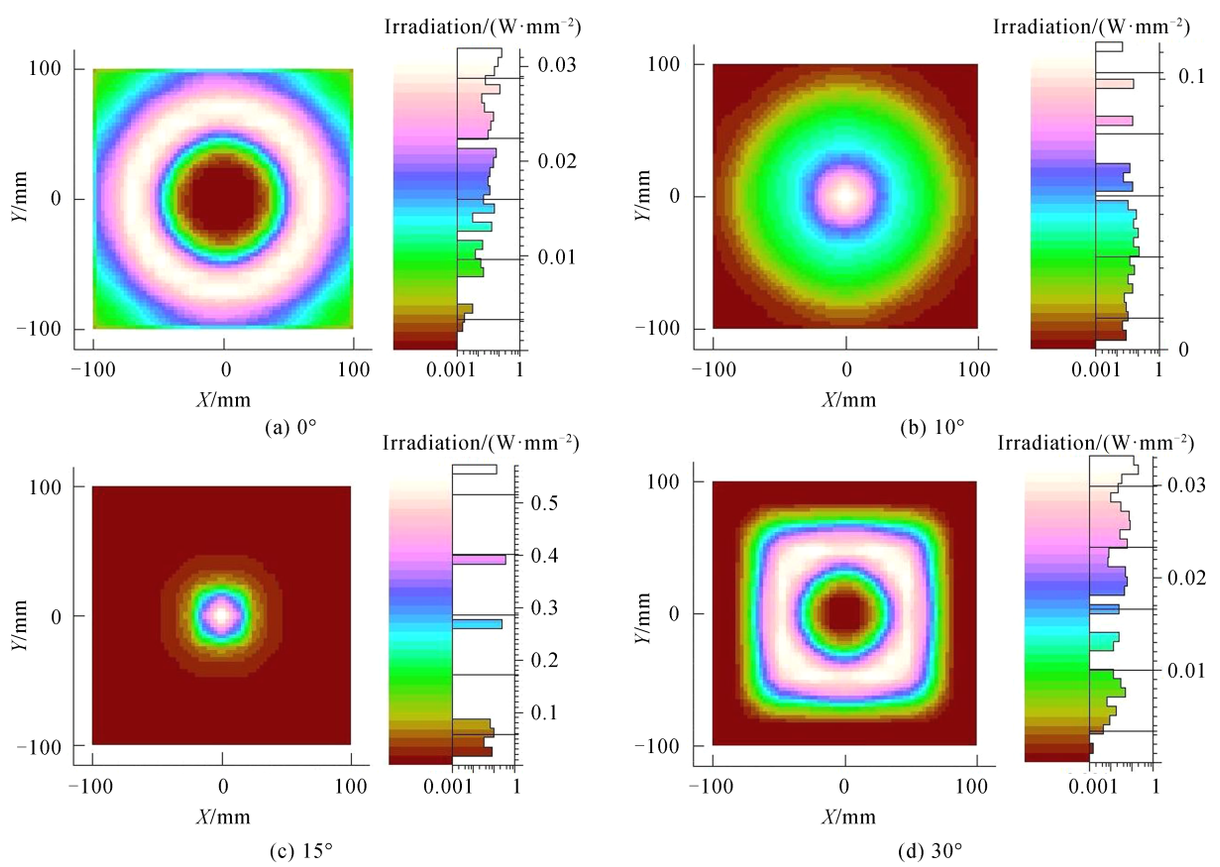

Fig. 6 Simulation results at various reception angles

The radiation flux of the receiving surface under each receiving angle was 960.9 W, 1 107 W, 1 070 W, and 399.2 W. Considering factors such as structure and irradiance, the CPC was designed with a maximum

acceptance angle of 15°.

Compared with the traditional condenser, the aspect ratio of the CPC was extremely large[14], and the mirror area was large as well. The upper mirror surface of the CPC was almost parallel to the symmetry axis. By intercepting part of the length, the structure could be simplified and the processing difficulty was reduced, without causing a significant condensing energy loss. As shown in Fig.7, the CPC and spherical condenser were ray-traced under different intercept ratios to analyze their effect on the light collection efficiency.

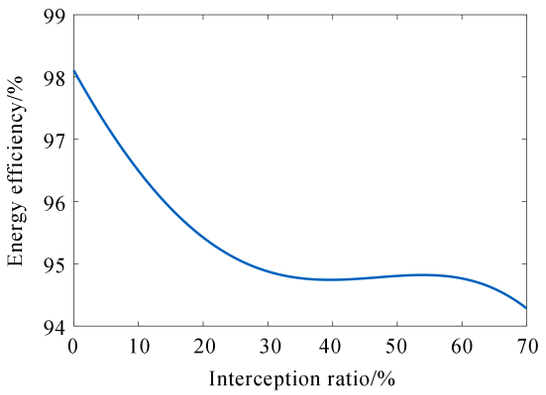

Fig. 7 Effect of the intercept ratio on light collection efficiency

Fig.7 shows that the efficiency of the concentrating system was still able to reach 94% after intercepting 70% of the CPC, indicating that the intercept ratio had little effect on the concentrating efficiency. The intercept ratio was set at 60% and the concentrating efficiency remained high, which solved the shortcomings of the CPC aspect ratio being extremely large.

3.3 Analysis of simulation results

After determining the CPC at the optimal intercept ratio, the light was traced in LightTools, and an irradiance image was obtained at the grid diameter of 50 mm on the receiving surface. As shown in Fig.8(a), from the grid data, the radiant flux received on the receiving plane was 1 921 W, and the calculated light collection efficiency reached 94.86%. The ellipsoidal condenser was then simulated under the same light source, the same working distance, and the same irradiation surface. As shown in Fig.8(b), the radiant flux on the receiving surface was 1 317 W, and the light collection efficiency was only 65%. These results indicated that the CPC-based light collection system had much higher light collection efficiency compared with the traditional light collector (ellipsoidal condenser)[15].

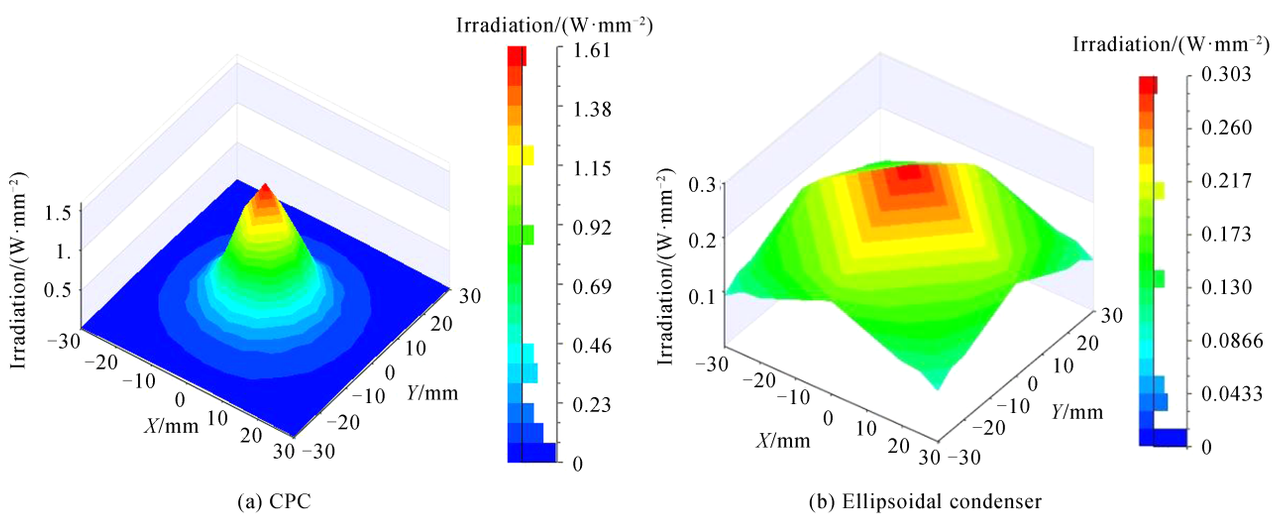

Fig. 8 Irradiance diagram of the receiving surface of CPC and ellipsoidal condenser

It can be seen from Table 1 that the CPC concentrating system had a great improvement in energy utilization compared with the traditional concentrating system.

Table 1 Performance simulation comparison between CPC combined concentrating system and ellipsoidal concentrating system

Structure	Radiant flux/W	Irradiation surface incident energy/W	Light source utilization/%
Single ellipsoidal mirror	2 025	1 317.2	65
CPC concentrating system	2 025	1 921	94.86

The overall simulation diagram of the solar simulator is shown in Fig.9. The raster chart of the irradiated surface is shown in Fig.10.

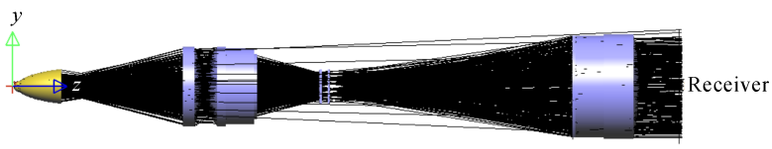

Fig. 9 Overall simulation diagram

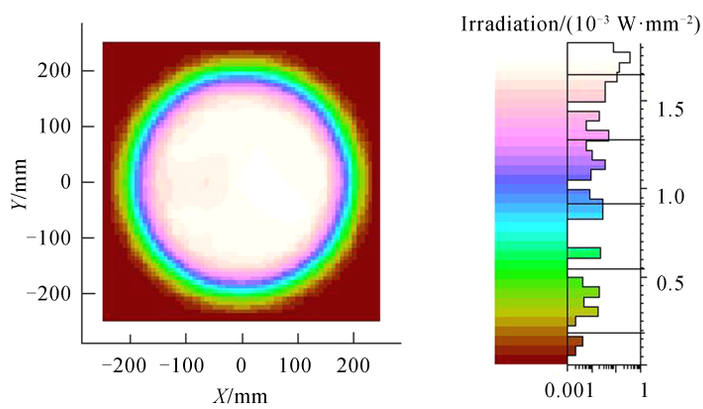

Fig.10 Irradiance raster chart

Fig. 10 shows that when the CPC was applied to the solar simulator, the improvement in the light collection efficiency also effectively improved the irradiance of the solar simulator.

4 Experimental verification

Regarding the solar simulator in the above design, the irradiance and irradiance uniformity tests were performed at a working distance of 2 m using an irradince meter. The experimental devices of the traditional and new solar simulators are shown in Fig.11.

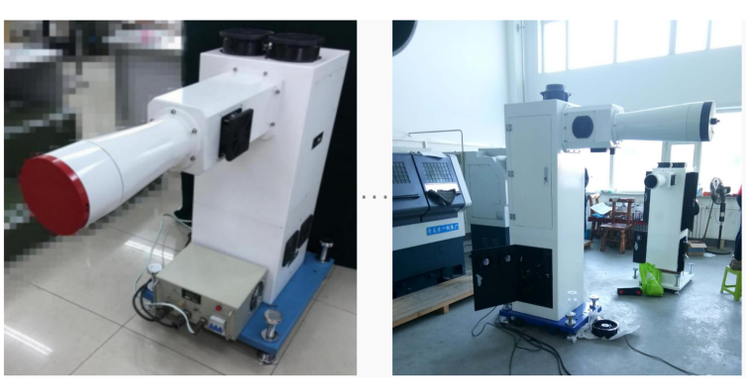

(a) Traditional solar simulator (b) New solar simulator

Fig.11 Experimental solar simulator device

Under the same power source two solar simulators were tested, a test grid was divided on the surface perpendicular to the optical axis. The grid diameter was 400 mm and a test point was set every 45° at the edge of the grid, for a total of eight edge test points and one center test point. The test data obtained subsequent to the measurements are listed in Table 2 below.

Table 2 Comparison of irradiance test data

Test point	Center point	1	2	3	4	5	6	7	8
Traditional solar simulator irradiance/($W \cdot m^{-2}$)	1 079	1 043	1 053	1 062	1 034	1 009	995	1 036	1 055
New solar simulator irradiance/($W \cdot m^{-2}$)	1 578	1 542	1 525	1 503	1 488	1 473	1 490	1 511	1 532

As shown in the table above, the highest irradiance at the center point was 1 578 W/m^2, whereas the lowest (at the fifth test point) was 1 473 W/m^2. The nonuniformity of irradiation was calculated as 3.4%. Experimental results were consistent with the simulation results.Compared with the traditional solar simulator, the new solar simulator had higher irradiance, which showed that the energy utilization was effectively improved.

5 Conclusion

This study proposed using a CPC to improve a solar simulator's concentrating system and to optimize the latter's overall design to achieve improvements in the solar simulator energy utilization and irradiance. First, the difference in the concentrating efficiency between the CPC and ellipsoidal condenser was analyzed, and the structural parameters were derived based on the working principle of the CPC. A nested model comprising a xenon lamp body light source and a CPC was established, and the irradiation distribution under different maximum receiving angles was analyzed to determine an ideal receiving angle of 15°. The light-collecting ability of the ellipsoidal mirror and the CPC was compared and analyzed. Simulation results showed that the energy utilization rate of the CPC and the spherical mirror was able to reach 94.86%, higher than that of the ellipsoidal condenser. When simplifying the CPC structure through interception, it was found that 60% interception had little effect on energy utilization and was beneficial to actual processing and manufacturing. Finally, the Monte Carlo method was applied to simulate the overall optical system of the solar simulator. Results delivered good irradiation results, the irradiance was verified to be higher by the test, and nonuniformity of irradiation reached 3.4%. Analysis results presented herein are conducive to the improvement of the overall efficiency of the solar simulator and provide new ideas for the design of high-irradiance solar simulators.

References

[1] BELLOS E, KORRES D, TZIVANIDIS C, *et al*. Design, simulation and optimization of a compound parabolic collector [J].*Sustainable Energy Technologies and Assessments*, 2016, **16**: 53-63.

[2] WANG Ya-xian, XU Wen-qing. Research on the key technology of shipboard LED search light [J]. *Optics & Optoelectronic Technology*, 2015, **13**(4): 70-74.

[3] ANDREEV V, KAZANTSEV A, KHVOSTIKOV V, *et al*.High-efficiency (24.6% AM 0) LPE grown AlGaAs/GaAs concentrator solar cells and modules [C]. Proceedings of 1994 IEEE 1st World Conference on Photovoltaic Energy Conversion - WCPEC, 1994, **2**: 2096-2099.

[4] HU Pian, LIU Yan, ZENG Shu-guang, *et al*.Effects of compound parabolic concentrator parameters on the concentration efficiency of solar lasers[J]. *Laser Journal*, 2017, **38**(10): 8-11.

[5] LI Li-feng, WANG Bao, POTTAS J, *et al*. Design of a compound parabolic concentrator for a multi-source high-flux solar simulator[J]. *Solar Energy*, 2019, **183**: 805-811.

[6] LIU Ling-zhi, LI Jian-hong. Research on optical analysis of compound parabolic concentrator (CPC) [J]. *Energy Technology*, 2006, (2): 52-56+59.

[7] LV Tao, ZHANG Jing-xu, FU Dong-hui, *et al*. Determination of parameters of ellipsoidal condenser in solar simulator[J]. *Journal of Applied Optics*, 2014, **35**(1): 43-47.

[8] WANG Le, ZHANG Shu-sheng, ZHAI Jing. Research on modeling of LED reflector based on compound parabolic concentrator[J]. *Laser & Optoelectronics Progress*, 2012, **49**(10): 159-164.

[9] WANG Fei, SUI Cheng-hua, YE Bi-qing. Research on the design parameters of compound parabolic concentrators [J]. *Optical Instruments*, 2010, **32** (3): 68-72.

[10] JIANG Lei. Design and research of Fresnel lens and compound parabolic concentrator[D]. Changchun: Jilin University,

2011.

[11] SONG Pei-yu. Design and simulation analysis of high collimation and high irradiance solar simulator[D]. Harbin: Harbin Institute of Technology, 2017.

[12] ESEN V, ŞSAĞLAM, ORAL B. Light sources of solar simulators for photovoltaic devices: A review[J]. *Renewable and Sustainable Energy Reviews*, 2017, **77**: 1240-1250.

[13] ABU-BAKAR S, MUHAMMAD-SUKKI F, FREIER D, *et al*. Performance analysis of a novel rotationally asymmetrical compound parabolic concentrator[J]. *Applied Energy*, 2015, **154**: 221-231.

[14] MA Ming, ZHENG Hong-fei, LI Jia-chun. The influence of the compound parabolic concentrator (CPC) truncation on its performance[J].*Solar Energy*, 2011,(7): 33-36.

[15] SUN Gao-fei, WANG Wen-peng, ZHANG Guo-yu, *et al*. Design and simulation of high irradiance multi-collimate angle solar simulation optical system[J]. *Acta Energiae Solaris Sinica*, 2018, **39**(8): 2209-2216.